Magn Reson Med Sci
doi:10.2463/mrms.mp.2021-0144 Published Online: March 17, 2022

MAJOR PAPER

Quantification of the Intrinsic T1 and T2 of Heschl's Gyri with MR Fingerprinting

Sho Maruyama[1], Sayuri Tatsuo[1], Soichiro Tatsuo[1], Saya Iida[1], Fumiyasu Tsushima[1], Satoru Ide[2], and Shingo Kakeda[1*]

Purpose: The human primary auditory cortex is located in the Heschl's gyrus (HG). To assess the intrinsic MR property in the gray matter of the HG (GM-HG) with T1 and T2 values using a commercially available MR fingerprinting (MRF) technique.

Methods: The subjects were 10 healthy volunteers (with 20 HGs; mean age, 31.5 years old; range, 25–53 years old). Coronal T1 and T2 maps were obtained with commercially available MRF using a 3-Tesla MR system. Two radiologists measured the T1 and T2 values of the GM-HG, the GM in the superior temporal gyrus (GM-STG), and the GM in the middle temporal gyrus (GM-MTG) by drawing a ROI on coronal maps.

Results: For both radiologists, the mean T1 and T2 values of the GM-HG were significantly lower than those in the GM-STG or GM-MTG ($P < 0.01$). The interobserver reliability using the intraclass correlation coefficients (ICC) (2,1) showed strong agreement for the measurement of the T1 and T2 values (ICCs = 0.80 and 0.78 for T1 and T2 values, respectively).

Conclusion: The T1 and T2 values on MRF for the GM-HG were lower than those for the GM-STG and GM-MTG, likely reflecting a higher myelin content and iron deposition in the GM-HG. Quantitative measurements using the MRF can clarify cortical properties with high reliability, which may indicate that MRF mapping provides new insights into the structure of the human cortical GM.

Keywords: *Heschl's gyrus, magnetic resonance fingerprinting, quantitative measurement, T1 map, T2 map*

Introduction

In clinical settings, the identification of the longitudinal relaxation time (T1) and transverse relaxation time (T2) may allow the collection of sensitive and complementary information about the tissue composition (macromolecules, lipid membranes, and iron) and water concentration.[1–3] Recently, Ma et al. proposed a novel imaging approach known as MR fingerprinting (MRF), which is capable of simultaneously obtaining multiple important tissue parameters from a single MRI scan.[4] MRF is based on the generation of unique signal signatures, termed as "fingerprints," for different tissue types based on their underlying MR properties. Matching the fingerprints to a database of simulated signals (dictionary) allows for parameter mapping of relaxation parameters, including T1, T2, and T2*.[5,6] Compared with other T1 and T2 mapping methods using conventional MRI approaches,[7–10] MRF is reported to have superior performance with regard to both accuracy and efficiency.[11] Recently, MRF became commercially available for joint T1 and T2 mapping.

In this study, we focused on the evaluation of intrinsic MR properties of Heschl's gyrus (HG) by the estimation of T1 and T2 by MRF because the intrinsic properties of the HG have been histopathologically and radiologically confirmed in many previous studies.[12–14] The human primary auditory cortex is located in the posterior part of the supratemporal plane. Anatomically, it largely corresponds with the transverse temporal gyri, or the HG.[12] Previous MR studies have reported the characteristic shape of the HG on sagittal or

[1]Department of Radiology, Hirosaki University Graduate School of Medicine, Hirosaki, Aomori, Japan
[2]Department of Radiology, University of Occupational and Environmental Health, School of Medicine, Kitakyushu, Fukuoka, Japan
[*]Corresponding author: Department of Radiology, Hirosaki University Graduate School of Medicine, 5, Zaifu-cho, Hirosaki, Aomori 036-8562, Japan. Phone: +81-172-33-5103, Fax: +81-172-33-5627, E-mail: kakeda@hirosaki-u.ac.jp

Received: November 7, 2021 | Accepted: January 12, 2022

coronal images;[13,14] the HG was anatomically identified as an Ω- or heart-shaped protrusion in the supratemporal plane in all subjects. Yoshiura et al. showed that the HG can be identified by the characteristic low signal intensity of its gray matter (GM) on T2-weighted imaging (T2WI) due to its myelin density and iron content.[15] Sigalovsky et al. found low T1 values in the posteromedial GM in the HG (GM-HG) based on its strong myelination.[16] Wasserthal et al. identified the GM-HG by combining two different complementary MR contrast modalities (T1- and T2-weighted anatomical imaging), which enhance the myelin density in the HG-GM.[17] Thus, quantitative measurements or evaluations of parameters by MRI may enable the identification of tissue properties (subtle cortical changes) that usually go unrecognized on vision inspection with conventional weighted MR images. However, their approach seems to require some complicated calculations and a long acquisition time. In this study, we evaluated the clinical usefulness of T1 and T2 values obtained with a commercially available MRF technique for the assessment of the intrinsic MR properties of the GM-HG.

Materials and Methods

Subjects

This study was approved by the institutional review board of our university hospital. Ten healthy volunteers (10 males, mean age 31.5 years old, and range 25–53 years old) participated in this study, and written informed consent was obtained before scanning. The study design was approved by an ethics review board. The healthy subjects had no history of neurological or psychiatric diseases. All subjects underwent coronal MRF and coronal R2* mapping in addition to routine brain MRI.

MRI

MRF was performed using a 3-Tesla MR scanner (MAGNETOM Vida; Siemens Healthcare, Erlangen, Germany) with a 64-channel head coil. We performed a 2D section-selective fast imaging with steady-state precession (FISP) – MRF sequence that generates T1 and T2 maps by matching measured signals to a set of simulated signals called a dictionary, as previously described.[5] 2D coronal MRF was scan with the following parameters: TR 12 ms; TE 2 ms; FOV, 256 mm; matrix, 256 × 256; slice thickness, 4 mm; resolution, 0.76 × 0.76 × 4 mm; bandwidth, 400000 Hz/pixel; number of slices, 34; acquisition time, 11 min 59 s. The B1 map was imaged before MRF since the MRF dictionary is calculated by performing the Bloch simulation for each combination of T1, T2, and B1 + parameters.

For quantitative study of brain iron content, R2* mapping has been used as a standard method.[18,19] Recent postmortem correlation studies have demonstrated that the relationship with R2* can be linear in regions of more uniform iron deposition.[20] Therefore, for the evaluation of iron contents in HG, we used R2* value as a reference standard. Technologically, in our institution, R2* mapping was not available using the 3-Tesla MR scanner (3T MAGNETOM Vida; Siemens). Therefore, R2* mapping was performed on a 3-Tesla MRI system (Signa EXCITE 3T; GE Healthcare, Chicago, IL, USA) using a dedicated eight-channel phased-array coil (USA Instruments, Aurora, OH, USA). R2* mapping was performed with a 3D flow-compensated multi-echo spoiled gradient echo (GRE) sequence. The imaging parameters included the coronal planes covering the brain, number of TE, 11; first TE, 4.5 ms; uniform TE spacing, 5 ms; TR, 58.4 ms; flip angle, 15°; bandwidth per pixel, ± 62.5 Hz; FOV, 22 × 16.5 cm; acquisition matrices, 320 × 416; slice thickness, 1.5 mm; and imaging time, 7 min 1 s.

Image interpretation

Image quality assessments

The MR images were reviewed in consensus by two neuroradiologists (S.K. with 24 years of experience and S.I. with 15 years of experience). For this study, 20 HGs in 10 healthy subjects were evaluated. The morphology of the auditory cortex has been described as highly variable, and there may be two or more HGs in a single hemisphere.[13] However, in this study, there were no subjects with complicated morphology of the auditory cortex. First, two neuroradiologists assessed the image quality of the coronal T1, T2, and R2* maps. For the depiction of the GM-HG, the following scores were used to describe the diagnostic value: 1, excellent; 2, adequate; and 3, nondiagnostic due to artifacts (Fig. 1). The radiologists were blinded to the MRI sequence and resolved all disagreements by a consensus reading of images.

ROI assessments

The HG was independently interpreted on the T1, T2, and R2* maps by two radiologists (F.T. with 20 years of experience and S.M. with 5 years of experience) according to the anatomical structures.[13,14] These images were always evaluated in conjunction with the conventional images (coronal T2WI or FLAIR). The radiologists then manually traced the ROIs of the GM-HG, which were always circular (1.25 mm^2), and placed them in the posteromedial GM-HG with histologically localized koniocortex[21,22] (Fig. 2). Using the ROI (1.25 mm^2), the GM in the superior temporal gyrus (GM-STG) and the GM in the middle temporal gyrus (GM-MTG) were also measured as references (Fig. 2).

Statistical analyses

From the T1 and T2 values, we calculated T1/T2 ratio. Differences with $P < 0.01$ were considered to be statistically significant. For the T1, T2, T1/T2 ratio, and R2* values, a paired t-test was used to calculate the statistical significance of the differences (GM-HG vs. GM-STG, GM-HG vs. GM-MTG). In the GM-HG, GM-STG, and GM-MTG, we also evaluated differences between the right and left hemispheres using a paired t-test. Results were corrected for multiple comparisons by a Bonferroni correction.

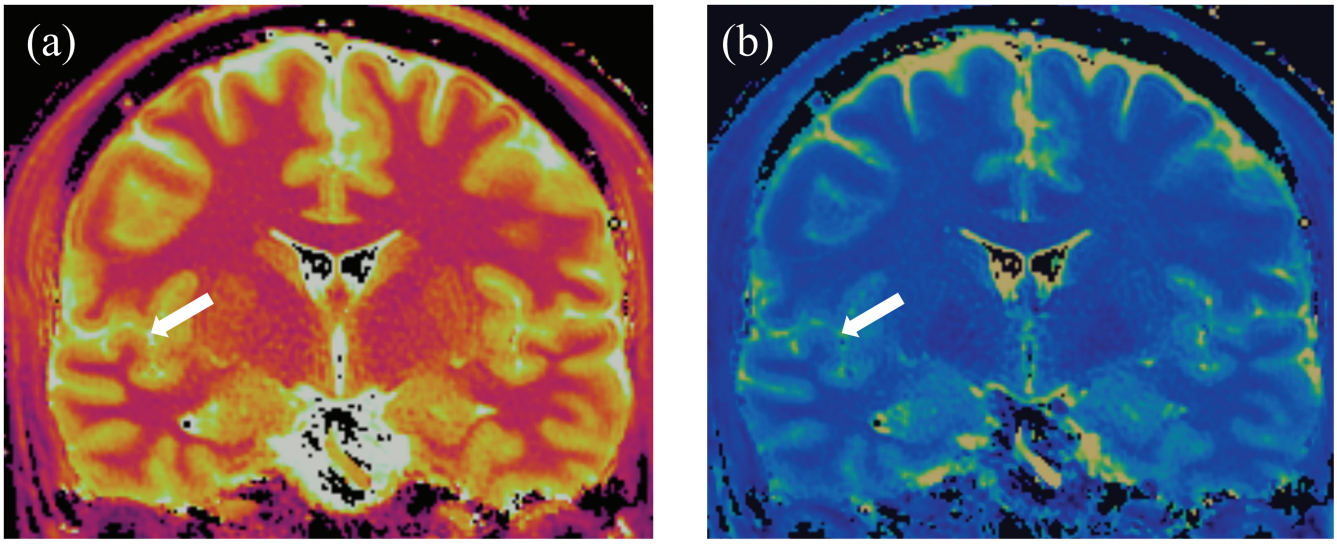

Fig. 1 A coronal T1 map (**a**) and T2 map (**b**) with MRF show Heschl's gyrus (arrows). MRF, MR fingerprinting.

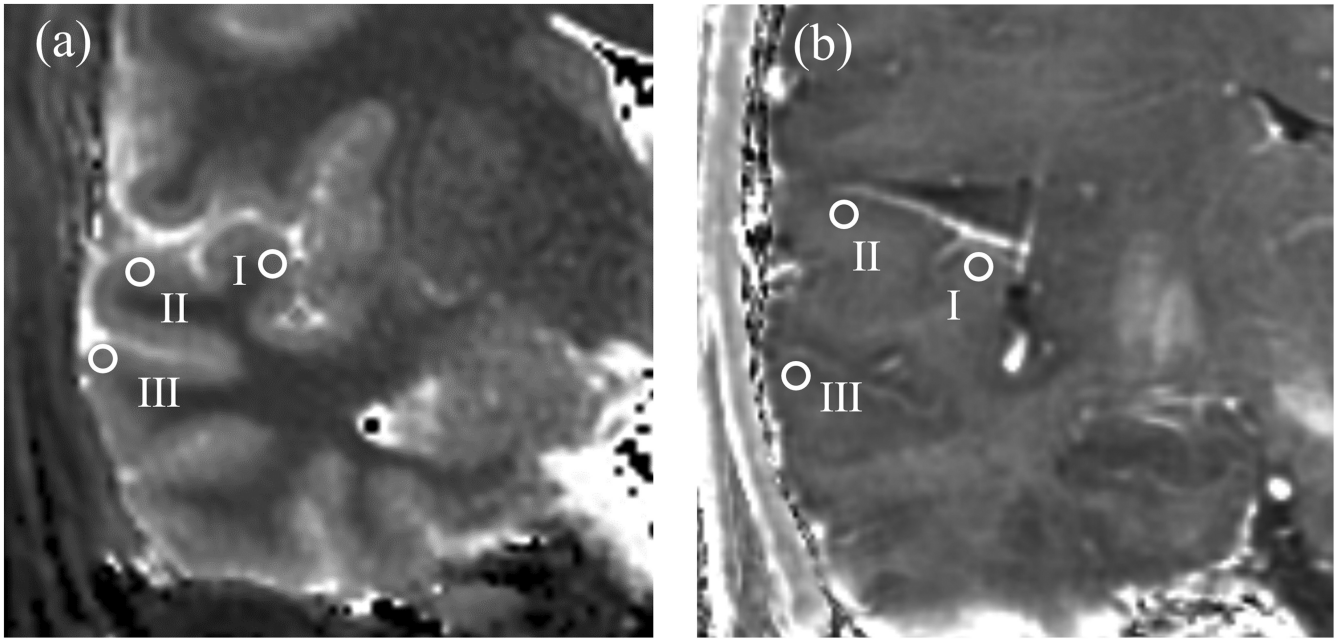

Fig. 2 Coronal T1 map with MRF (**a**) and R2* map (**b**) show the ROIs used in the quantitative analysis: (I) Heschl's gyrus, (II) superior temporal gyrus, (III) middle temporal gyrus. MRF, MR fingerprinting.

The interobserver reliability in ROI placement for the quantitative measurements (T1, T2, and R2* values) by two radiologists was assessed using intraclass correlation coefficients (ICCs), with ICC (2,1) 0–0.2 indicating poor agreement, 0.3–0.4 fair agreement, 0.5–0.6 moderate agreement, 0.7 0.8 strong agreement, and > 0.8 excellent agreement.[23]

All statistical analyses were conducted using the R software program (CRAN, freeware), and the ICCs were analyzed using the formula of Shrout et al.[24]

Results

Image quality assessments

For the depiction of the GM-HG, GM-STG, and GM-MTG, all images (T1 and T2 maps) obtained with MRF were scored as excellent on both sides of all 10 subjects (100%, 20/20), whereas the R2* maps were scored as either excellent (75%, 15/20) or adequate (25%, 5/20).

Table 1 Measurements of T1, T2, and R2* values

		Radiologist 1			Radiologist 2			ICC(2,1)
		GM-HG	GM-STG	GM-MTG	GM-HG	GM-STG	GM-MTG	
MRF	T1 value (ms)	1336.0 (46.4)	1464.8 (47.7)**	1499.0 (39.3)**	1338.5 (40.0)	1436.8 (46.2)**	1521.3 (43.0)**	0.80
	T2 value (ms)	51.4 (4.34)	60.0 (4.46)**	62.6 (4.50)**	49.4 (5.25)	60.5 (3.62)**	63.2 (5.08)**	0.78
	T1/T2 ratio	26.2 (2.41)	24.5 (1.75)**	24.1 (1.56)**	27.4 (2.99)	23.8 (1.32)**	24.2 (1.60)**	
R2* value (1/sec)		18.6 (1.19)	16.4 (0.75)**	15.2 (0.82)**	18.0 (0.84)	16.4 (0.68)**	15.2 (0.84)**	0.68

Data are average value or ratio ± standard deviation. **Significantly different from GM-HG ($P < 0.01$). GM, gray matter; HG, Heschl's gyrus; ICC, intraclass correlation coefficient; MRF, MR fingerprinting; MTG, middle temporal gyrus; STG, superior temporal gyrus.

Table 2 Comparison of right and left HG

		Radiologist 1		*P* value	Radiologist 2		*P* value
		right GM-HG	left GM-HG		right GM-HG	left GM-HG	
MRF	T1 value (ms)	1341.5 (42.2)	1330.4 (52.0)	0.55	1340.5 (25.9)	1336.4 (51.9)	0.81
	T2 value (ms)	51.5 (4.79)	51.3 (4.09)	0.92	50.4 (6.04)	48.4 (4.41)	0.33
	T1/T2 ratio	26.3 (2.73)	26.1 (2.18)	0.79	26.9 (3.32)	27.8 (2.72)	0.31
R2* value (1/sec)		18.2 (0.79)	19.0 (1.41)	0.16	17.7 (0.67)	18.3 (0.90)	0.11

Data are average value or ratio ± standard deviation. GM, gray matter; HG, Heschl's gyrus; MRF, MR fingerprinting.

ROI assessments

For radiologist 1, the mean T1 (ms) and T2 (ms) values in the GM-HG were significantly lower than those in the GM-STG (1336.0 ± 46.4 vs. 1464.8 ± 47.7 for T1 value, $P < 0.01$; 51.4 ± 4.34 vs. 60.0 ± 4.46 for T2 value, $P < 0.01$) and GM-MTG (1336.0 ± 46.4 vs. 1499.0 ± 39.3 for T1 value, $P < 0.01$; 51.4 ± 4.34 vs. 62.6 ± 4.50 for T2 value, $P < 0.01$) (Table 1). The mean T1/T2 ratio and R2* (1/sec) values in the GM-HG were significantly higher than those in the GM-STG (26.2 ± 2.41 vs. 24.5 ± 1.75 for T1/T2 ratio, $P < 0.01$; 18.6 ± 1.19 vs. 16.4 ± 0.75 for R2* values, $P < 0.01$) and GM-MTG (26.2 ± 2.41 vs. 24.1 ± 1.56 for T1/T2 ratio, $P < 0.01$; 18.6 ± 1.19 vs. 15.2 ± 0.82 for R2* values, $P < 0.01$) (Table 1).

Regarding each average measurement (T1 value, T2 value, T1/T2 ratio, and R2* value) in the GM-HG, GM-STG, and GM-MTG, there was no significant difference between the right and left hemispheres (Table 2).

The interobserver reliability assessed using the ICC (2,1) showed strong agreement for the measurement of the T1 and T2 value (ICCs = 0.80 and 0.78 for T1 and T2 values, respectively) and moderate agreement for the R2* value (ICCs = 0.68).

Discussion

We found that the mean T1 and T2 values in the GM-HG, which were measured by two different radiologists, were significantly lower than those in the GM-STG and the GM-MTG. Regarding the R2* values, the mean value in the GM-HG was significantly higher than that in the GM-STG and GM-MTG. The interobserver reliability showed strong agreement for the measurement of T1 and T2 values. Based on the histological features described in a previous report, our results may reflect the iron content[25] and degree of myelination in GM-HG.[7,16,21,26]

Recent reports demonstrated the utility of T1 and T2 mappings by MRF to discover focal cortical pathologies. T1 value of cortical GM on T1 map discriminated patients with Parkinson's disease from controls with sensitivity 83.3% and specificity 88.0%.[27] Keil et al. showed that T1 values in cortical GM were significantly longer in patients with frontotemporal lobe degenerative dementia than in controls.[28] In the previous epilepsy studies, MRF-based T1 and T2 maps showed potential to identify epileptogenic lesions from the patients with negative conventional MRI diagnosis.[29,30] For predicting outcomes after mild traumatic brain injury, T1 value in GM was found to have higher utility than fractional anisotropy and apparent diffusion coefficient from diffusion tensor imaging.[31] Our study is in line with these previous studies and our results may emphasize that information from MRF is a promising new MRI tool to distinguish microstructural differences in GM.

The T1 value of a given brain voxel is determined by the physical properties of its underlying tissue and is mainly dependent on the free water content, iron content, and total

amount of tissue components and concentrations and types of macromolecules (e.g. degree of myelination).[10] Based on previous studies, we suspect that this is one of the reasons that the low T1 value of GM-HG might reflect its heavy myelination. Our ROIs were placed in the posteromedial GM-HG with histologically localized koniocortex.[21,22] The koniocortex is an area of especially heavy myelination.[32,33] T1 values are highly correlated with myelin content in the spinal cord[34] and brain.[35,36] Although, to our knowledge, there are no combined quantitative MR and quantitative histology studies directly assessing the T1/myelin correlation in cortical GM, there is no a priori reason to expect this relationship to be different. Using R1 (the reciprocal of T1)-derived myelin mapping techniques, Lutti et al. were able to identify the auditory core as the medial-to-lateral decreased area in R1.[37] Sigalovsky et al. found that the temporal lobe regions with high R1 values on spatial mappings of R1 always overlapped with the posteromedial GM-HG, including the koniocortex.[16] These previous studies support our results, where the mean T1 values in the GM-HG were significantly lower than those in the GM-STG and GM-MTG.

The brain normally contains several essential metals. Iron is the most frequently encountered paramagnetic substance in the healthy brain and is normally present in concentrations sufficient to affect MR images.[38] Many previous studies have reported T2 shortening in the motor cortex in older neurologically normal subjects[39–41] due to the magnetic susceptibility effect produced by iron deposition in the brain. Hallgren and Sourander[42] reported that iron staining was observed more often in the motor cortex than in the other cortices. Importantly, a quantitative biochemical study showed that the iron content of the auditory cortex was comparable to that of the motor.[25] This report is consistent with our present finding, where the mean T2 values in the GM-HG were significantly lower than those in the GM-STG and GM-MTG. Furthermore, as well as R2* value, we observed increased T1/T2 values in the GM-HG, which may also indicate the accumulation of iron.[7] In contrast, T2-shortening effect does not be reflected only by the iron deposition, heavy myelination may also contribute to T2 shortening. Water trapped between the myelin layers has a shorter T2 value (20 ms) than that in the intra- and extracellular compartments (80 ms).[43] A high concentration of myelin would therefore lead to relatively short T2 values. Thus, the relatively short T2 values in the GM-HG in this study may have been due to heavy myelination of the GM-HG.

MRF has several advantages over other MRI approaches,[7–10] allowing for superior quantification. Since the quantification of T1 and T2 values is obtained simultaneously using MRF, the effects of motion between scans are mitigated. In addition, multiple system parameters, such as B0 and B1 field inhomogeneity, can also be incorporated into MR signal models so that accurate quantification can be obtained even in the presence of system imperfections.[44] MRF is also less sensitive to subject motion than other approaches. This is partly due to the usage of a non-Cartesian spiral readout, leading to better performance in the presence of motion than with a conventional Cartesian readout. Moreover, the template-matching algorithm also helps mitigate the noise-like motion artifacts and thus improves motion tolerance when using MRF.[4] Therefore, for the measurements with MRF, there is no misregistration between the T1 and T2 maps due to subject and/or scan motions. These advantages with MRF are further supported by our results; the interobserver reliability using the ICC (2,1) showed strong agreement with regard to the T1 and T2 values. Although many studies have used an axial plane with MRF, we used coronal MRF images and found high reliability for the quantification of T1 and T2 values. Our results suggest that MRF might be feasible as a diagnostic tool in various neuro-imaging studies, as many important brain structures, such as the hippocampus, hypothalamic nucleus, and substantia nigra, are depicted more accurately on the coronal plane than on the axial plane.

The previous study with young healthy subjects showed that the volume of the HG was larger in the left hemisphere than in the right,[14] which might be related to the known left-hemisphere dominance for speech. Furthermore, another investigator demonstrated that inter-hemispheric comparisons revealed a greater R1 value in the left HG than in the right HG, suggesting greater GM myelination in the left auditory cortex.[16] However, we found no significant difference between the right and left hemispheres. The negative result may be due to the lower spatial resolution with MRF than with the previous method (R1 map).[16] Indeed, our spatial resolution with MRF was $0.76 \times 0.76 \times 4.0$ mm, whereas that of the R1 map in the previous study was $1.3 \times 1.0 \times 1.3$ mm. Therefore, further studies with GM-HG using MRF with a high spatial resolution will be needed in larger samples.

Several limitations associated with the present study warrant mention. Our study population was small, and we evaluated only normal young adults. Further investigations may be needed to determine whether or not MRF can depict a disease that affects the GM-HG. In this study, we could not directly evaluate myelin content. Although the previous study showed that the MRF enabled quantitative measures of myelin water fraction in human brain,[45] we could obtain only T1 and T2 maps from the commercially available MRF.

Conclusion

Our results revealed that the T1 and T2 values of the GM-HG with MRF were lower than those of the GM-STG and GM-MTG, likely due to the higher myelin content and iron deposition. We found that the T1 and T2 measurements obtained with MRF demonstrated excellent interobserver agreement, indicating that MRF is a reliable tool for quantitative measurement of the brain tissue properties (subtle cortical changes).

These results indicate that MRF mapping *in vivo* can provide new insights into the structure of the human cortical GM.

Conflicts of Interest

The authors declare that they have no conflicts of interest.

References

1. Callaghan MF, Helms G, Lutti A, Mohammadi S, Weiskopf N. A general linear relaxometry model of R1 using imaging data. Magn Reson Med 2015; 73:1309–1314.
2. Stüber C, Morawski M, Schäfer A, et al. Myelin and iron concentration in the human brain: a quantitative study of MRI contrast. Neuroimage 2014; 93:95–106.
3. Saito N, Sakai O, Ozonoff A, Jara H. Relaxo-volumetric multispectral quantitative magnetic resonance imaging of the brain over the human lifespan: global and regional aging patterns. Magn Reson Imaging 2009; 27:895–906.
4. Ma D, Gulani V, Seiberlich N, et al. Magnetic resonance fingerprinting. Nature 2013; 495:187–192.
5. Jiang Y, Ma D, Seiberlich N, Gulani V, Griswold MA. MR fingerprinting using fast imaging with steady state precession (FISP) with spiral readout. Magn Reson Med 2015; 74:1621–1631.
6. Rieger B, Zimmer F, Zapp J, Weingärtner S, Schad LR. Magnetic resonance fingerprinting using echo-planar imaging: Joint quantification of T1 and relaxation times. Magn Reson Med 2017; 78:1724–1733.
7. Bonnier G, Fischi-Gomez E, Roche A, et al. Personalized pathology maps to quantify diffuse and focal brain damage. Neuroimage Clin 2019; 21:101607.
8. Boto J, Askin NC, Regnaud A, et al. Cerebral gray and white matter involvement in anorexia nervosa evaluated by T1, T2, and T2* mapping. J Neuroimaging 2019; 29:598–604.
9. Hashido T, Saito S. Quantitative T1, T2, and T2* mapping and semi-quantitative neuromelanin-sensitive magnetic resonance imaging of the human midbrain. PLoS One 2016; 11:e0165160.
10. Nürnberger L, Gracien R-M, Hok P, et al. Longitudinal changes of cortical microstructure in Parkinson's disease assessed with T1 relaxometry. Neuroimage Clin 2016; 13:405–414.
11. Körzdörfer G, Kirsch R, Liu K, et al. Reproducibility and repeatability of MR fingerprinting relaxometry in the human brain. Radiology 2019; 292:429–437.
12. Liegeois-Chauvel C, Musolino A, Chauvel P. Localization of the primary auditory area in man. Brain 1991; 114(Pt1A):139–151.
13. Yousry T, Fesl G, Buttner A, Noachtar S, Schmid U. Heschl's gyrus-Anatomic description and methods of identification on magnetic resonance imaging. Int J Neuroradiol 1997; 3:2–12.
14. Penhune VB, Zatorre R, MacDonald J, Evans A. Interhemispheric anatomical differences in human primary auditory cortex: probabilistic mapping and volume measurement from magnetic resonance scans. Cereb Cortex 1996; 6:661–672.
15. Yoshiura T, Higano S, Rubio A, et al. Heschl and superior temporal gyri: low signal intensity of the cortex on T2-weighted MR images of the normal brain. Radiology 2000; 214:217–221.
16. Sigalovsky IS, Fischl B, Melcher JR. Mapping an intrinsic MR property of gray matter in auditory cortex of living humans: a possible marker for primary cortex and hemispheric differences. Neuroimage 2006; 32:1524–1537.
17. Wasserthal C, Brechmann A, Stadler J, Fischl B, Engel K. Localizing the human primary auditory cortex in vivo using structural MRI. Neuroimage 2014; 93 Pt 2: 237-251.
18. Ordidge RJ, Gorell JM, Deniau JC, Knight RA, Helpern JA. Assessment of relative brain iron concentrations using T2-weighted and T2*-weighted MRI at 3 Tesla. Magn Reson Med 1994; 32:335–341.
19. Haacke EM, Cheng NY, House MJ, et al. Imaging iron stores in the brain using magnetic resonance imaging. Magn Reson Imaging 2005; 23:1–25.
20. Langkammer C, Krebs N, Goessler W, et al. Quantitative MR imaging of brain iron: a postmortem validation study. Radiology 2010; 257:455–462.
21. Morosan P, Rademacher J, Schleicher A, Amunts K, Schormann T, Zilles K. Human primary auditory cortex: cytoarchitectonic subdivisions and mapping into a spatial reference system. Neuroimage 2001; 13:684–701.
22. Rademacher J, Morosan P, Schormann T, et al. Probabilistic mapping and volume measurement of human primary auditory cortex. Neuroimage 2001; 13:669–683.
23. Landis JR, Koch GG. The measurement of observer agreement for categorical data. Biometrics 1977:159–74.
24. Shrout PE, Fleiss JL. Intraclass correlations: uses in assessing rater reliability. Psychol Bull 1979; 86:420–428.
25. Höck A, Demmel U, Schicha H, Kasperek K, Feinendegen L. Trace element concentration in human brain. Activation analysis of cobalt, iron, rubidium, selenium, zinc, chromium, silver, cesium, antimony and scandium. Brain 1975; 98:49–64.
26. Yoshiura T, Higano S, Rubio A, et al. Heschl and superior temporal gyri: low signal intensity of the cortex on T2-weighted MR images of the normal brain. Radiology 2000; 214:217–221.
27. Keil VC, Bakoeva SP, Jurcoane A, et al. A pilot study of magnetic resonance fingerprinting in Parkinson's disease. NMR Biomed 2020; 33:e4389.
28. Keil VC, Bakoeva SP, Jurcoane A, et al. MR fingerprinting as a diagnostic tool in patients with frontotemporal lobe degeneration: A pilot study. NMR Biomed 2019; 32:e4157.
29. Ma D, Jones SE, Deshmane A, et al. Development of high-resolution 3D MR fingerprinting for detection and characterization of epileptic lesions. J Magn Reson Imaging 2019; 49:1333–1346.
30. Liao C, Wang K, Cao X, et al. Detection of lesions in mesial temporal lobe epilepsy by using MR fingerprinting. Radiology 2018; 288:804–812.
31. Gerhalter T, Cloos M, Chen AM, et al. T1 and T2 quantification using magnetic resonance fingerprinting in mild traumatic brain injury. Eur Radiol 2022; 32:1308–1319.
32. Hackett TA, Preuss TM, Kaas JH. Architectonic identification of the core region in auditory cortex of macaques, chimpanzees, and humans. J Comp Neurol 2001; 441:197–222.
33. Wallace MN, Johnston PW, Palmer AR. Histochemical identification of cortical areas in the auditory region of the human brain. Exp Brain Res 2002; 143:499–508.

34. Mottershead J, Schmierer K, Clemence M, et al. High field MRI correlates of myelin content and axonal density in multiple sclerosis. J Neurol 2003; 250:1293–1301.
35. Schmierer K, Scaravilli F, Altmann DR, Barker GJ, Miller DH. Magnetization transfer ratio and myelin in postmortem multiple sclerosis brain. Ann Neurol 2004; 56:407–415.
36. Schmierer K, Wheeler-Kingshott CA, Tozer DJ, et al. Quantitative magnetic resonance of postmortem multiple sclerosis brain before and after fixation. Magn Reson Med 2008; 59:268–277.
37. Lutti A, Dick F, Sereno MI, Weiskopf N. Using high-resolution quantitative mapping of R1 as an index of cortical myelination. Neuroimage 2014; 93:176–188.
38. Schenck JF, Zimmerman EA. High-field magnetic resonance imaging of brain iron: birth of a biomarker? NMR Biomed. 2004; 17:433–445.
39. Kakeda S, Korogi Y, Kamada K, et al. Signal intensity of the motor cortex on phase-weighted imaging at 3T. Am J Neuroradiol 2008; 29:1171–1175.
40. Kamada K, Kakeda S, Ohnari N, Moriya J, Sato T, Korogi Y. Signal intensity of motor and sensory cortices on T2-weighted and FLAIR images: intraindividual comparison of 1.5 T and 3T MRI. Eur Radiol 2008; 18:2949–2955.
41. Hirai T, Korogi Y, Sakamoto Y, Hamatake S, Ikushima I, Takahashi M. T2 shortening in the motor cortex: effect of aging and cerebrovascular diseases. Radiology 1996; 199:799–803.
42. Hallgren B, Sourander P. The effect of age on the non-haemin iron in the human brain. J Neurochem 1958; 3:41–51.
43. Laule C, Leung E, Li DK, et al. Myelin water imaging in multiple sclerosis: quantitative correlations with histopathology. Mult Scler J 2006; 12:747–753.
44. Chen Y, Jiang Y, Pahwa S, et al. MR fingerprinting for rapid quantitative abdominal imaging. Radiology 2016; 279:278–286.
45. Chen Y, Chen M-H, Baluyot KR, Potts TM, Jimenez J, Lin W. MR fingerprinting enables quantitative measures of brain tissue relaxation times and myelin water fraction in the first five years of life. Neuroimage 2019; 186:782–793.